Journal of Inflammation Research Dovepress

Open Access Full Text Article ORIGINAL RESEARCH

Unveiling Key Biomarkers and Mechanisms in Septic Cardiomyopathy: A Comprehensive Transcriptome Analysis

Dandan Zhao[1,2,*], Jinqiang Zhuang[3,*], Liping Wang[4], Lili Wu[5], Wangjie Xu[6], Lu Zhao[4], Jiang Hong[1], Wei Jin[1], Congliang Miao[1]

[1]Department of Internal and Emergency Medicine, Shanghai General Hospital, Shanghai Jiao Tong University School of Medicine, Shanghai, People's Republic of China; [2]Department of Emergency Medicine, Affiliated Hospital of Xuzhou Medical University, Xuzhou, People's Republic of China; [3]Department of Emergency Intensive Care Unit (EICU), Affiliated Hospital of Yangzhou University, Yangzhou, People's Republic of China; [4]Jiangsu Key Laboratory of New Drug Research and Clinical Pharmacy, Xuzhou Medical University, Xuzhou, People's Republic of China; [5]Department of Cardiology, Shanghai Songjiang District Central Hospital, Shanghai, People's Republic of China; [6]Laboratory Animal Center, Instrumental Analysis Center, Shanghai Jiao Tong University, Shanghai, People's Republic of China

*These authors contributed equally to this work

Correspondence: Congliang Miao; Wei Jin, Department of Internal and Emergency Medicine, Shanghai General Hospital, Shanghai Jiao Tong University School of Medicine, Shanghai, People's Republic of China, Email mcl15917908206@163.com; jw1230123@126.com

Purpose: Septic cardiomyopathy (SCM) is a significant global public health concern characterized by substantial morbidity and mortality, which has not been improved for decades due to lack of early diagnosis and effective therapies. This study aimed to identify hub biomarkers in SCM and explore their potential mechanisms.

Methods: We utilized the GSE53007 and GSE207363 datasets for transcriptome analysis of normal and SCM mice. Hub biomarkers were identified through a protein–protein interaction (PPI) network and validated using LPS-treated C57/BL6 mice. Functional enrichment analysis was performed to uncover relevant signaling pathways, while single-cell RNA sequencing was used to examine key genes and regulatory mechanisms associated with SCM.

Results: A total of 374 differentially expressed genes (DEGs) were identified, with 268 genes up-regulated and 106 genes down-regulated. Functional enrichment highlighted chemokine activity and receptor binding, with KEGG pathways revealing significant involvement of the TNF and IL-7 signaling pathways. Deterioration of cardiac function, elevated inflammatory markers such as IL-1β, IL-6, and increased cardiac injury biomarkers such as cTnI indicated the successful establishment of our SCM model. Subsequently, qPCR was conducted to validate the expression of the top 10 genes, through which we identified Cd40, Tlr2, Cxcl10, Ccl5, Cxcl1, Cd14, Gbp2, Ifit2, and Vegfa as key biomarkers. Single-cell sequencing indicated increased neutrophil and macrophage populations, with decreased B cells and cardiomyocytes. Additionally, transcription regulators Irf1 and Stat1 were found to potentially regulate the expression of Gbp2, Cxcl10, Ccl5, and Cd40, linking SCM to immune response, ferroptosis, pyroptosis, cuproptosis, and m6A RNA methylation modification.

Conclusion: This study identified nine hub biomarkers and two transcription regulators associated with SCM. Exploring the connections between SCM and immunity, ferroptosis, pyroptosis, cuproptosis, and m6A RNA methylation might provide insights into the underlying mechanisms. These findings enhanced our understanding of SCM's underlying mechanisms and might pave the way for novel therapeutic strategies to improve clinical outcomes.

Keywords: septic cardiomyopathy, integrated bioinformatics analysis, hub biomarkers, single-cell data analysis, immunity

Introduction

Severe sepsis is a noteworthy factor of the mortality in intensive care units and has become a primary cause of death in both developed and developing nations.[1] Septic cardiomyopathy (SCM), an acute cardiac impairment that arises from sepsis, is a remediable condition that could be managed at the initial stages of sepsis. Despite extensive research aimed at

Received: 12 July 2024
Accepted: 14 December 2024
Published: 23 December 2024

comprehending the molecular mechanism of septic cardiomyopathy, a precise characterization and prognostic indicators remain elusive.[2] Therefore, it is vital to identify the underlying genes and effective biomarkers in SCM for early diagnosis, prevention, and intervention.[3] SCM is a pathophysiological syndrome caused by infection, so identifying the targeted infection is crucial to minimizing mortality and morbidity. Previous studies found that the substances such as lipopolysaccharides (LPS), prostanoids, cytokines, the complement system, and nitric oxide, which might be involved in impaired cardiac function.[3]

Since the advent of bioinformatics technology, studying the function and regulatory mechanisms of genes has become a mainstream approach to treating diseases.[4,5] Gene Expression Omnibus (GEO) is an open database containing many gene expression profiles of different diseases.[6] This database serves as a valuable resource for conducting gene expression analysis, functional analysis, and identifying differentially expressed genes (DEGs) relevant to SCM. Although previous research has already identified numerous biomarkers for SCM, but these studies did not perform experimental verification and used only bioinformatics analysis, and did not explore the relationship between SCM and immunity or programmed cell death.[7,8] In this research, we identified the hub genes and transcription factors, and investigated the interconnections between SCM and various biological processes, including immunity, ferroptosis, pyroptosis, cuproptosis and m6A RNA methylation, providing a platform for future research into its potential mechanisms.

Material and Methods

Data Collection and Processing

GEO (https://www.ncbi.nlm.nih.gov/gds) is a public database for high throughput gene sequencing. We selected GSE53007 datasets as our research object. Differently expressed genes (DEGs) were determined by *p*-value and fold change (FC) and the thresholds were set as adjusted P (fdr) < 0.05 and |log2 FC| ≥1 in this article. All data were downloaded online in public.

Functional Enrichment Analysis

We used the "clusterProfiler" R package to conduct enrichment analysis of Kyoto Encyclopedia of Genes and Genomes (KEGG) pathways and gene ontology (GO) functional categories, including cellular components, molecular functions, and biological processes. Enrichment analysis based on DEGs was beneficial for us to discover the pathogenesis of SCM and we also applied bubble plots to visualize these results.

Protein–Protein Interaction (PPI) Network Construction

In order to study the relationship between these genes, we analyzed and visualized the PPI network through the STRING (https://string-db.org/) online website based on DEGs of SCM. STRING database was used to predict the PPI network of DEGs and analyze the interactions between proteins.[9]

Random Forest (RF) and Extreme Gradient Boosting (XGBoost) Mode Construction and Hub Gene Identification

The Random Forest (RF) learning method integrated the outcomes of numerous decision trees that were generated through bootstrap sampling of the training dataset, and randomly selects a subset of predictors from the entire set of properties in each tree.[10] The present study's implementation of the RF method was based on prior research.[11] The Extreme Gradient Boosting (XGBoost) technique relied on a sparsity-aware algorithm and a weighted quantile sketch, wherein the weak learners were sequentially converged into an ensemble to produce a strong learner.[12]

Transcription Factor Identification

The TRRUST (https://www.grnpedia.org/trrust/) database is a valuable resource for predicting transcriptional regulatory networks in human and mouse, provides insight into the regulation of these interactions.[13] As soon as the validated genes

have been screened into TRRUST, we would query the interaction between genes and transcription factors, build networks, and display them using Cytoscape.

Single-Cell Sequencing and Analysis

We chosed GSE207363 as the focus of our research from the GEO database. The methodology described in a published article[14] was followed to implement the Seurat package. The Anchors function of the Seurat R package was used to integrate the sepsis data package. Initially, the Seurat package was employed for quality control and standardization. Subsequently, Principal Component Analysis (PCA) was performed to tackle the difficulties arising from the high dimensionality of the expression matrix. The dimensionality reduction and visualization technique known as Uniform Manifold Approximation and Projection (UMAP) was utilized in this study. Specific marker genes for each cell subtype were identified by selecting those with an absolute average log2FC greater than 1 and a *p*_val_adj less than 0.05. Manual annotation of cell clusters was performed to differentiate between various cell types sourced from the PanglaoDB database (https://panglaodb.se/). In our study, we employed a set of well-defined gene markers to accurately classify various cell types. Specifically, we utilized Adgre1, Fcgr1 and Cd68 gene markers for the classification of macrophages, Pecam1, Vwf and Emcn gene markers for the classification of endothelial cells, Col1a1 and Col1a2 gene markers for the classification of fibroblasts, Tnni3, Mb and Myl3 gene markers for the classification of cardiomyocytes, S100a9, S100a8 and Mki67 gene markers for the classification of neutrophils, Cd79a and Igkc gene markers for the classification of B cells, Acta2 and Myh11 gene markers for the classification of smooth muscle cells, and Cd3g, Gzma and Ccl5 gene markers for the classification of NK/T cells, Rgs5 and Kcnj8 gene markers for the classification of pericytes, and Kcna2, Ank3, and Chl1 gene markers for the classification of neurons.

Construction of Sepsis-Induced Myocardial Injury Mouse Model

The present study was approved by Animal Ethics Committee of Shanghai General Hospital (Shanghai, China). A total of 20 C57/BL6 male mice (age, 8 weeks weight, 24 ± 2g) were obtained from the Laboratory Animal Center of Shanghai General Hospital (Shanghai, China). All mice were kept in a pathogen-free laboratory environment under controlled temperature (23 ± 1°C) and 65%–70% relative humidity. Mice were divided into two groups as follows: control group and lipopolysaccharide (LPS) treatment group. The mice of LPS group were injected intraperitoneally with LPS at a dosage of 10 mg/kg body weight, and the mice from control group injected intraperitoneally with normal saline. The mice were sacrificed 36 h after LPS treatment, and their hearts were collected for further study.

Echocardiographic Measurements

Transthoracic echocardiography was performed using a VEVO 3000. Mice were anesthetized with isoflurane (1.5% to 1% in air), shaved with the use of depilatory cream, and placed on a dedicated heating plate in the supine position. During the procedure, heart rate and temperature (35–37°C) were monitored. Two-dimensional parasternal long-axis views at the level of the largest LV diameter were obtained for guided B-mode and M-mode measurements at the end of the diastole and systole. Endocardium contours were drawn from end-systolic and end-diastolic long-axis views; LV end diastolic and -systolic volumes were measured, and the percentage ejection fraction (EF) was then calculated.

Enzyme-Linked Immunosorbent Assay (ELISA)

The concentrations of IL-1β, IL-6 and cTnI in mouse plasma were detected using ELISA by commercial kits (Abclonal, China). Briefly, antibodies against IL-1β, IL-6, and cTnI were immobilized on 96-well plates and incubated with pretreated samples for 2 hours. Subsequently, conjugate antibody and HRP-conjugated anti-mouse immunoglobulin were added separately and incubated for 1 hour. After washing, a TMB substrate solution was added for 30 minutes to stop the reaction. Finally, a spectrophotometer was used to detect the absorbance at 450 nm.

Haematoxylin and Eosin (HE) Staining

After immersing the heart in 4% paraformaldehyde, dehydrated it, and embedded it in paraffin, the next step is to section the tissue embedded in paraffin. The sections were placed in xylene, and then ethanol (for dewaxing and rehydration). HE staining proceeded as instructed by the kit manufacturer (Beyotime). The images were stained with haematoxylin for

10 minutes, washed with water to remove excess solution, stained with eosin for 2 minutes, dehydrated with ethanol and xylene, and observed after mounting.

Immunohistochemistry (IHC) Assay

Initially, the excised heart was treated with paraformaldehyde for fixation, followed by dehydration and embedding in paraffin. Subsequently, the paraffin-embedded tissue would be subjected to sectioning. Lastly, the tissue sections underwent a series of procedures including deparaffinization, hydration, antigen retrieval, endogenous peroxidase blocking, blocking, antibody incubation, DAB staining, nuclear staining, and dehydration. The antibody of IL-1β came from Cell Signaling Technology (Danvers, MA, USA) and the antibody of IL-6 came from Affinity.

The Extraction of RNA and Quantitative Real-Time Polymerase Chain Reaction

We grinded frozen hearts repeatedly in a tissue homogenizer. RNAiso Plus reagent (Takara Bio, Japan) was utilized to extract RNA according to the manufacturer's instructions. The extracted RNA was converted into cDNA by the use of the PrimeScript™ RT Master Mix (Perfect Real Time) Kit (Takara Bio, Japan). Quantitative realtime PCR (qPCR) experiments were performed on a Quantstudio 6 flex Real-Time PCR System using SYBR Green (Takara Bio, Japan). The expression level of 10 differentially expressed genes and 6 transcription factor genes were normalized to GAPDH expression levels and presented in $2^{-\Delta\Delta CT}$ between the two groups. These primer sequences were designed and synthesized by Sangon Biotech Co., Ltd. (Shanghai, China), and the sequences were shown in Supplementary Tables 1 and 2.

Western Blotting

Western blotting was performed as follows. In brief, samples were lysed in RIPA sample buffer, lysates were separated by SDS–PAGE, and proteins were electrotransferred to an Immobilon-p polyvinylidene fluoride (PVDF) membrane. Membranes were blocked for 2 hours at room temperature with 5% nonfat dry milk in TBS-T buffer and then incubated overnight at 4°C with the indicated primary antibodies (All the antibodies were purchased from Abclonal). Subsequently, membranes were washed 3×10 minutes in TBS-T, incubated with appropriate horseradish peroxidase (HRP)-conjugated secondary antibodies for 2 hours at room temperature, and then washed 3×5 minutes in TBS-T. An ECL detection system (Tanon, China) was used to visualize protein bands.

A Study of the Association Between SCM and Immune Cell Infiltration, Immune Microenvironment, Immune Checkpoint Molecules, Ferroptosis, Pyroptosis, Cuproptosis and m6A RNA Methylation

In terms of immunity, three aspects were examined, including immune cell infiltration, immune microenvironment, and immune checkpoint molecules. In order to determine the level of immune cell infiltration from gene expression data, Newman developed an analytical tool, CIBERSORT, that relies on gene expression data.[15] We used the ESTIMATE algorithm to analysis the immune microenvironment including StromalScore, ImuneScore, and EstimateScore.[16] In addition, different expressions of immune checkpoint molecules, ferroptosis, cuproptosis, pyroptosis and m6A evaluation in control and SCM groups were also displayed by R package 'limma'.

Statistical Analysis

The data and figures of this paper were conducted by SPSS 23.0 software (SPSS, Chicago, IL, USA) and GraphPad Prism 8.0 (San Diego, CA, USA). Bioinformatics analysis was analyzed by R 4.1.1 software. All *p*-values were two-sided and statistics would be significant if $p < 0.05$.

Results

Data Processing and Acquisition of DEGs in SCM

In this research, we selected GSE53007 dataset from the GEO database for further data analysis, GSE53007 was derived from mice and consisted of four normal mouse heart tissue samples and four SCM mouse heart tissue samples. The flow

chart of the study design was shown in Figure 1. Based on the thresholds of adjusted *P* (fdr) < 0.05 and |log2 FC| ≥ 1 in this article, a total of 374 DEGs were identified in SCM, including 268 up-regulated and 106 down-regulated genes. Furthermore, we have also selected out the representative 100 differently expressed genes, including 50 up-regulated genes and 50 down-regulated genes. The Volcano plots for genes and expression heatmaps for DEGs were shown in Figure 2A and B. Moreover, all of these up- and down-regulated genes were detailed in Supplementary Tables 3 and 4.

PPI Network Based on DEGs and Functional Enrichment Analysis in SCM

Based on DEGs of SCM, the PPI network was analyzed and visualized through the STRING online website to study the relationships between these genes (Figure 2C). Based on the highest connectivity degrees in the PPI network, the top 30 genes were selected as hub biomarkers in SCM (Figure 2D). The GO enrichment analysis DEGs into three groups: biological processes group (BP), cellular component group (CC), and molecular function group (MF). As shown in Figure 2E, in the biological processes group, the DEGs were mainly enriched in cytokine-mediated signaling pathway, response to lipopolysaccharide response to virus, response to molecule of bacterial origin and others. In the cellular component group, the DEGs were mainly enriched in membrane microdomain, collagen-containing extracellular matrix, receptor complex and so on. In the molecular function group, the DEGs were mainly enriched in chemokine activity, chemokine receptor binding, cytokine activity, cytokine receptor binding, CXCR and CCR chemokine receptor-binding et al. As shown in Figure 2F, KEGG pathways were mainly enriched in the TNF signaling pathway, IL-7 signaling pathway, cytokine–cytokine receptor interaction, NF-kappa B signaling pathway, Toll-like receptor signaling pathway and so on. Detailed statistical information for all data was given in Supplementary Tables 5 and 6.

Identification of the Hub Genes by RF and XGB Model

In order to develop a diagnostic gene signature related to SCM, RF and XGB models were constructed independently. The residual distribution for the RF model was found to be lower than that of the XGB model, as evidenced by the boxplots displaying the |residual| and reverse cumulative distribution of |residual| values (Figure 3A and B). Based on these findings, the RF model was deemed more suitable for predicting the occurrence of SCM, and was therefore selected for further analysis. Using the RF learning method, we identified 10 genes. The correlation and heat maps were presented in Figure 3C and D.

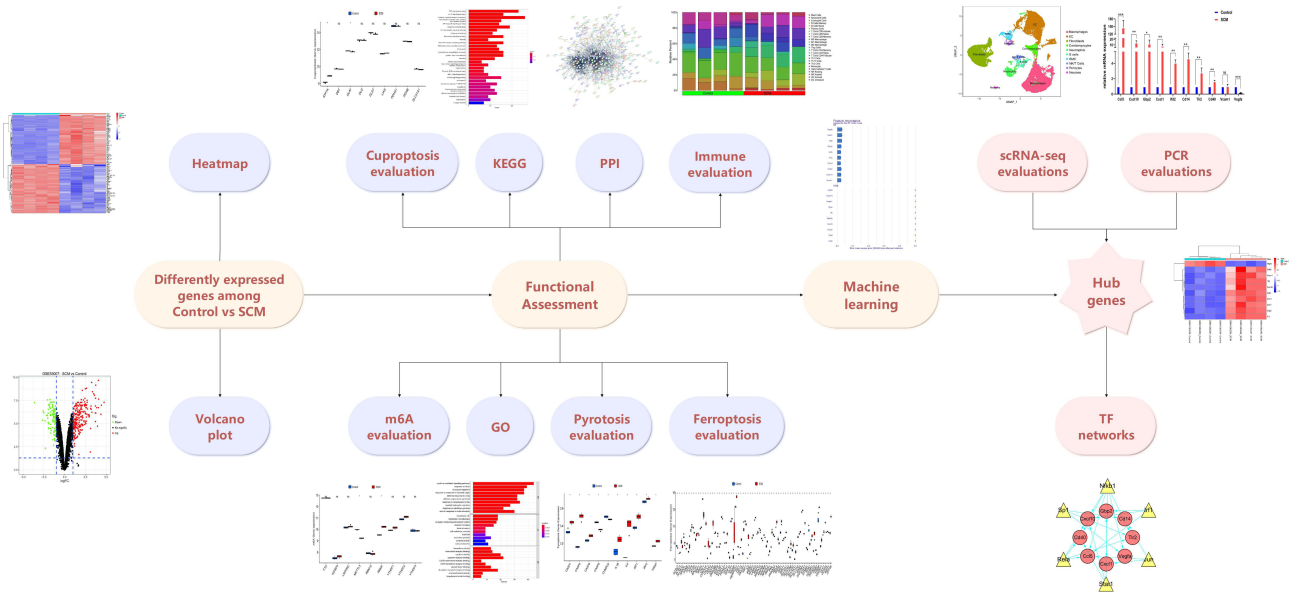

Figure 1 The flow chart of the study.

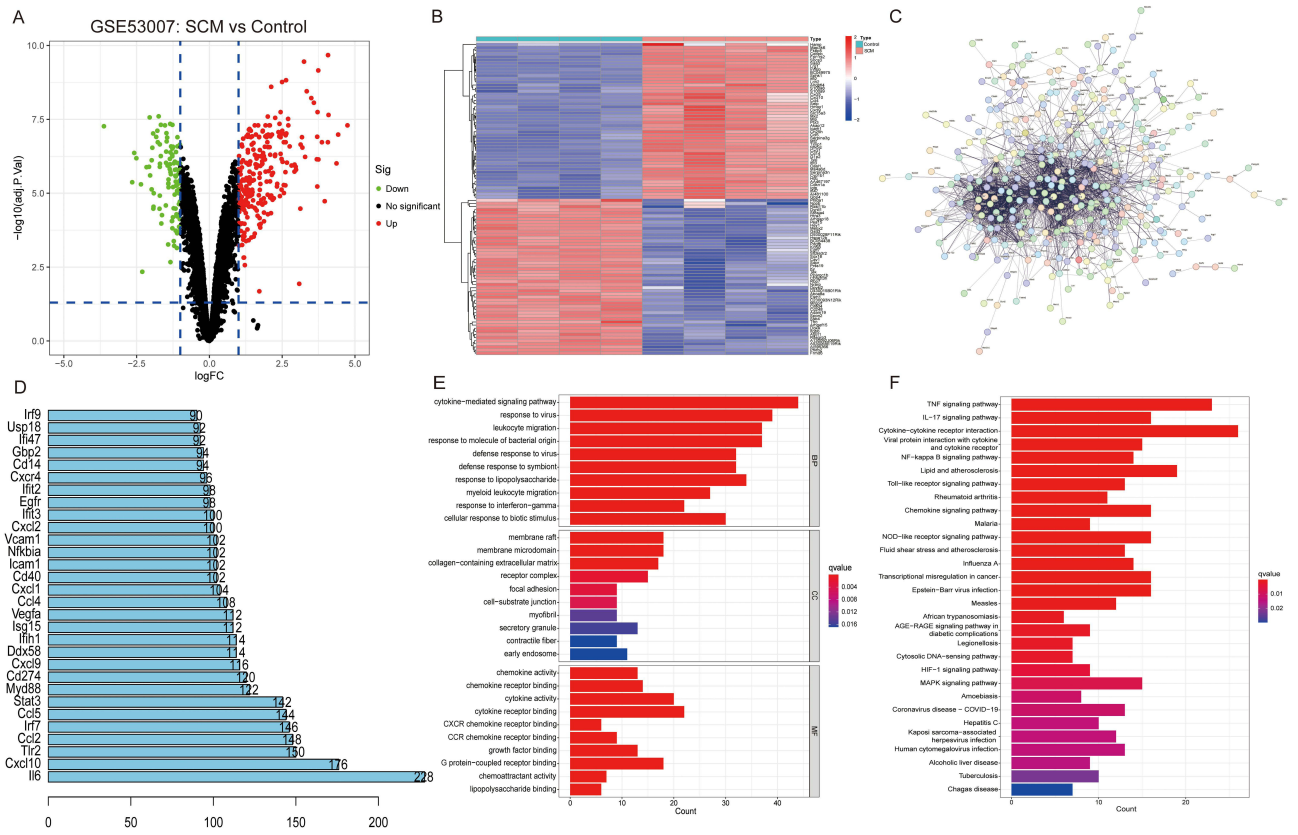

Figure 2 Data processing and acquisition of (DEGs) and PPI network based on DEGs and functional enrichment analysis in SCM; (**A**) Volcano plot of the DEGs in the GSE53007 dataset. (**B**) Heatmap of the DEGs in the GSE53007 dataset. (**C**) PPI network; (**D**) The top 30 genes with the highest connectivity degrees in the PPI network; (**E**) Gene ontology (GO) enrichment analysis; (**F**) KEGG enrichment analysis.

Successful Establishment of the Murine SCM Model

Firstly, we used HE staining to observe the cardiac pathological changes between the control group and LPS-treated group. HE staining results indicated that there were no obvious histopathological changes in the myocardial tissues of mice in the control group, the myocardial tissues were in clear striations, with no edema, degeneration and atrophy. In contrast, apparent pathological changes occurred in the myocardial tissues of model: there were obvious disorganization of cardiac muscles, edema, cell necrosis and fibroelastosis. (Figure 4A and B). IL-1β and IL-6, which were commonly recognized as typical inflammatory markers in acute inflammation, were assessed for their expression in both the control and SCM groups through immunohistochemical analysis. The results revealed a significant increase in the expression levels of IL-1β and IL-6 within the SCM group when compared to the control group (Figure 4C-H). Secondly, we used ELISA Kits to evaluate the expressions of related inflammatory factors and myocardial injury biomarker. As shown in Figure 4I-K, the plasma levels of IL-1β, IL-6, and cTnI in the SCM group were significantly elevated. Lastly, the echocardiogram indicated a higher EF in the SCM group compared to the control group (Figure 4L-N). These findings provided additional evidence supporting the successful establishment of the SCM mouse model.

Quantitative Real-Time PCR Validations of Hub Biomarkers for SCM

The expressions of these top 10 genes in the GSE53007 dataset, which were selected based on their highest connectivity degrees in the PPI network, were visually represented in Figure 5A. The top ten hub genes, namely Ccl5, Cxcl10, Gbp2, Cxcl1, Ifit2, Cd14, Tlr2, Cd40, Vcam1, and Vegfa, exhibited differential regulation, with Vegfa being the only down-regulated gene, while the others were up-regulated (Figure 5A). To validate the expression of these identified genes, quantitative real-time PCR (qPCR) was employed. The results depicted in Figure 5B demonstrated that nine out of the

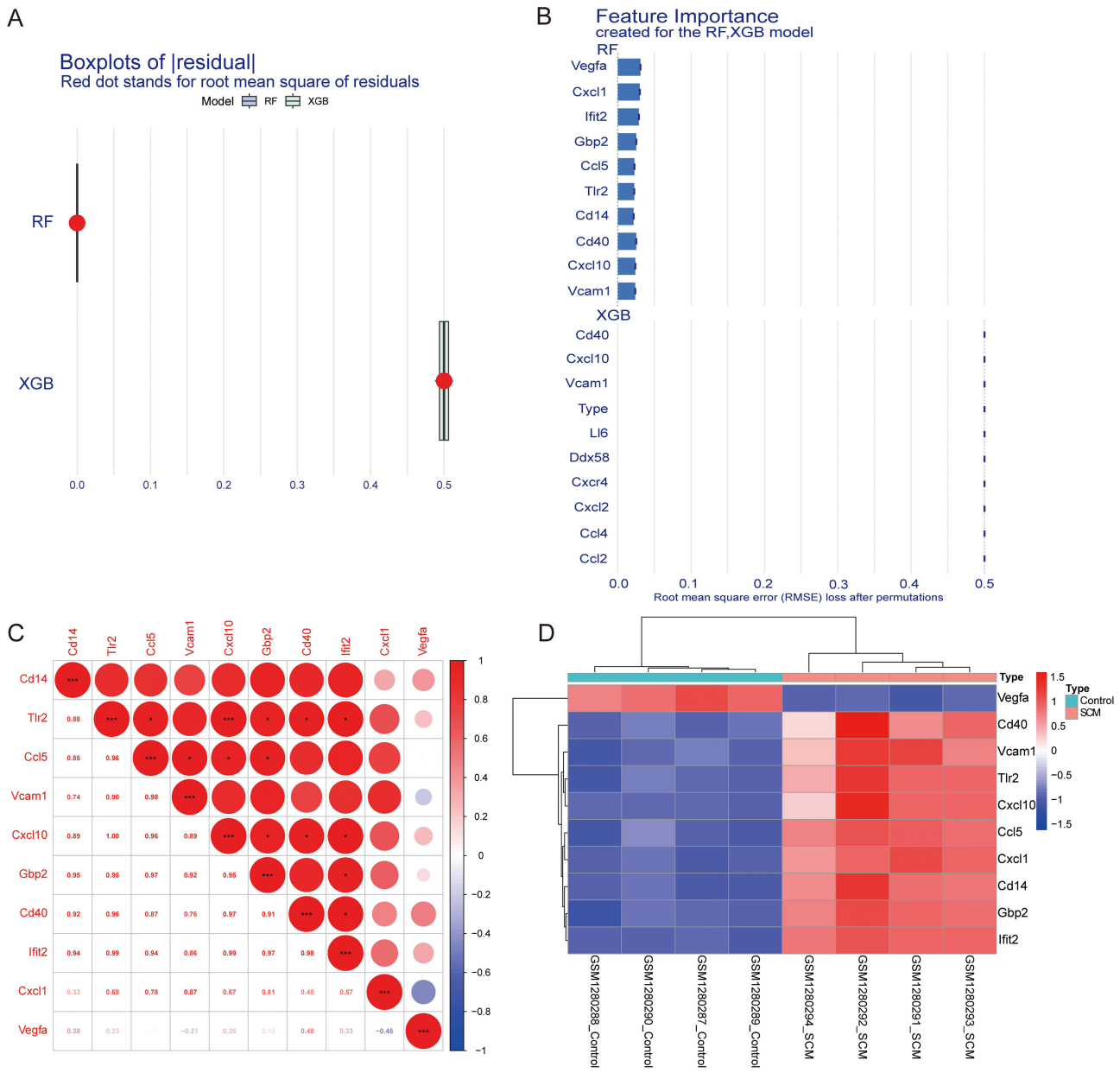

Figure 3 Construction of the RF model and XGBoost model and identification of the hub genes. (**A**) The residual for the RF model and XGB model. (**B**) Identification of the hub genes by RF and XGB model. (**C**) The correlation map of hub genes. (**D**) The heat maps of hub genes.

ten genes exhibited distinct expression patterns between the SCM and control groups. Furthermore, these nine genes exhibited expression trends consistent with those observed in the GSE53007 dataset (Figure 5B).

Single-Cell mRNA Sequencing Data

In order to further evaluate the hub gene expression in immune cells and predict the response to immunotherapy, we analyzed the single-cell sequencing data of sepsis. Notably, as shown in GSE207363, total of 10 major cell types, comprising macrophages, endothelial cells (EC), fibroblasts, cardiomyocytes, neutrophils, B cells, smooth muscle cells (SMC), NK/T cells, pericytes, neurons, were identified based on the canonical gene marker expressions. Based on the examination of single-cell data plots, our research revealed that sepsis-induced myocardial injury was characterized by an elevation in neutrophil and macrophage populations, while B cell and cardiomyocyte counts decrease. (Figure 6A). These findings implied a plausible correlation between sepsis and compromised immune system functionality. Consequently, we

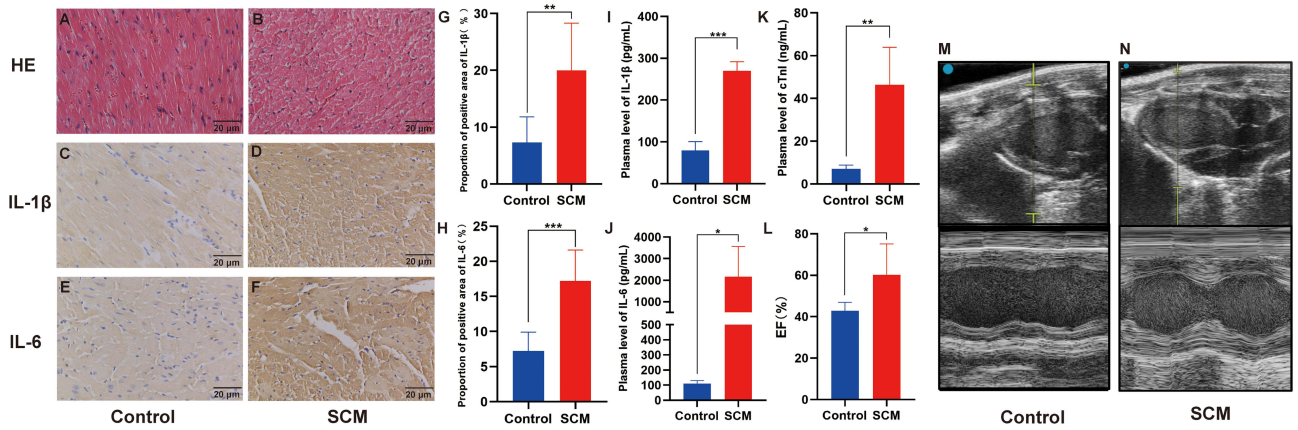

Figure 4 Successful establishment of the murine SCM model. (**A** and **B**) Histopathological images of HE-stained heart in control and SCM groups. (**C** and **D**) The expression of IL-1β in control and SCM groups; (**E** and **F**) The expression of IL-6 in control and SCM groups. (**G** and **H**) Bar graph of IL-1β and IL-6 immunohistochemical staining; (**I**) Plasma level of IL-1β; (**J**) Plasma level of IL-6; (**K**) Plasma level of cTnI; (**L**) Percentage ejection fraction; (**M**) Echocardiogram (B-mode and M-mode) of the control group; (**N**) Echocardiogram (B-mode and M-mode) of the SCM group. Scale bar: 20 μm. *p < 0.05; **p < 0.01; ***p < 0.001.

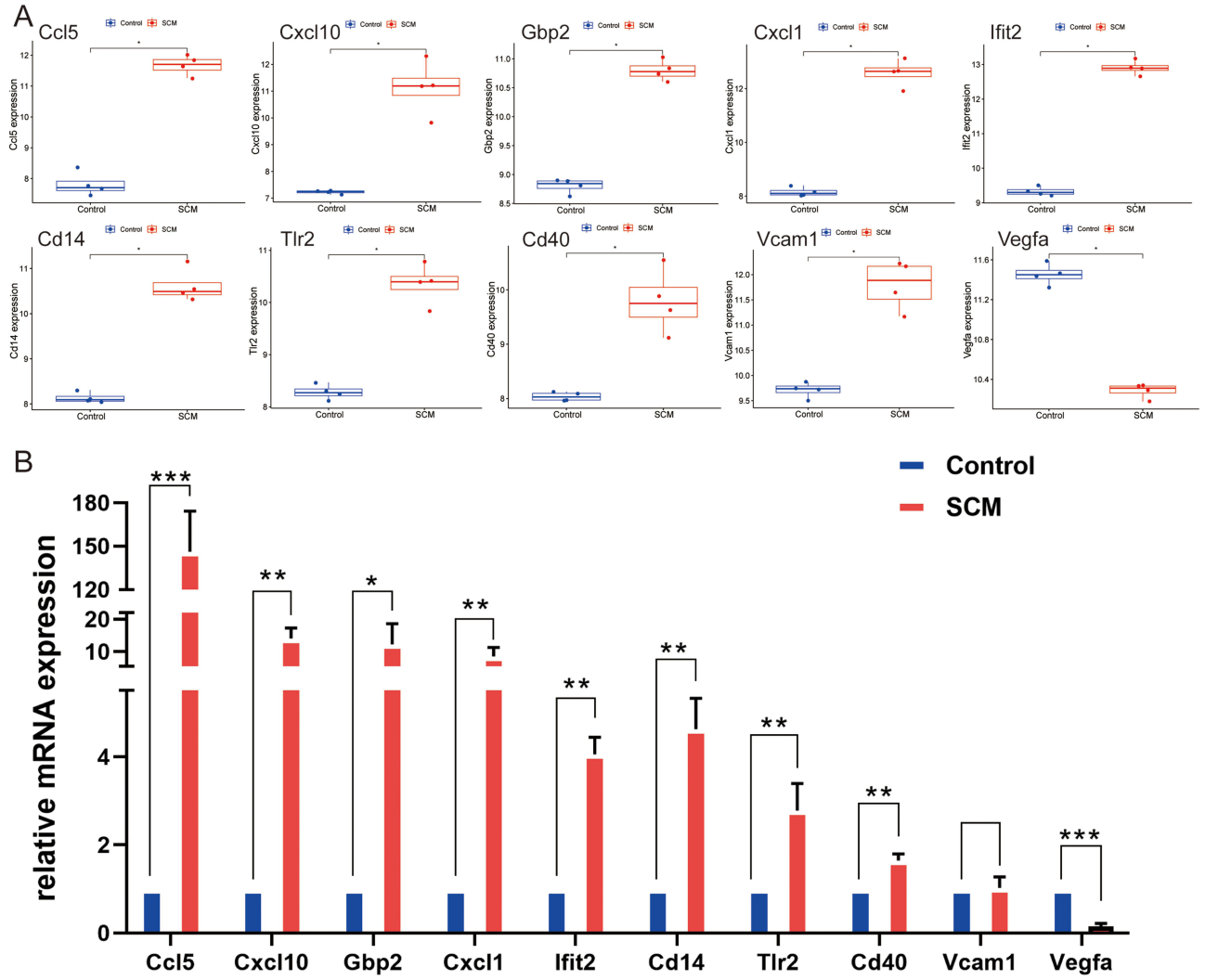

Figure 5 qPCR validations of hub biomarkers for SCM; (**A**) Expression of these top ten genes in the GSE53007 dataset; (**B**) Validations of these top ten genes by qPCR. *p < 0.05; **p < 0.01; ***p < 0.001.

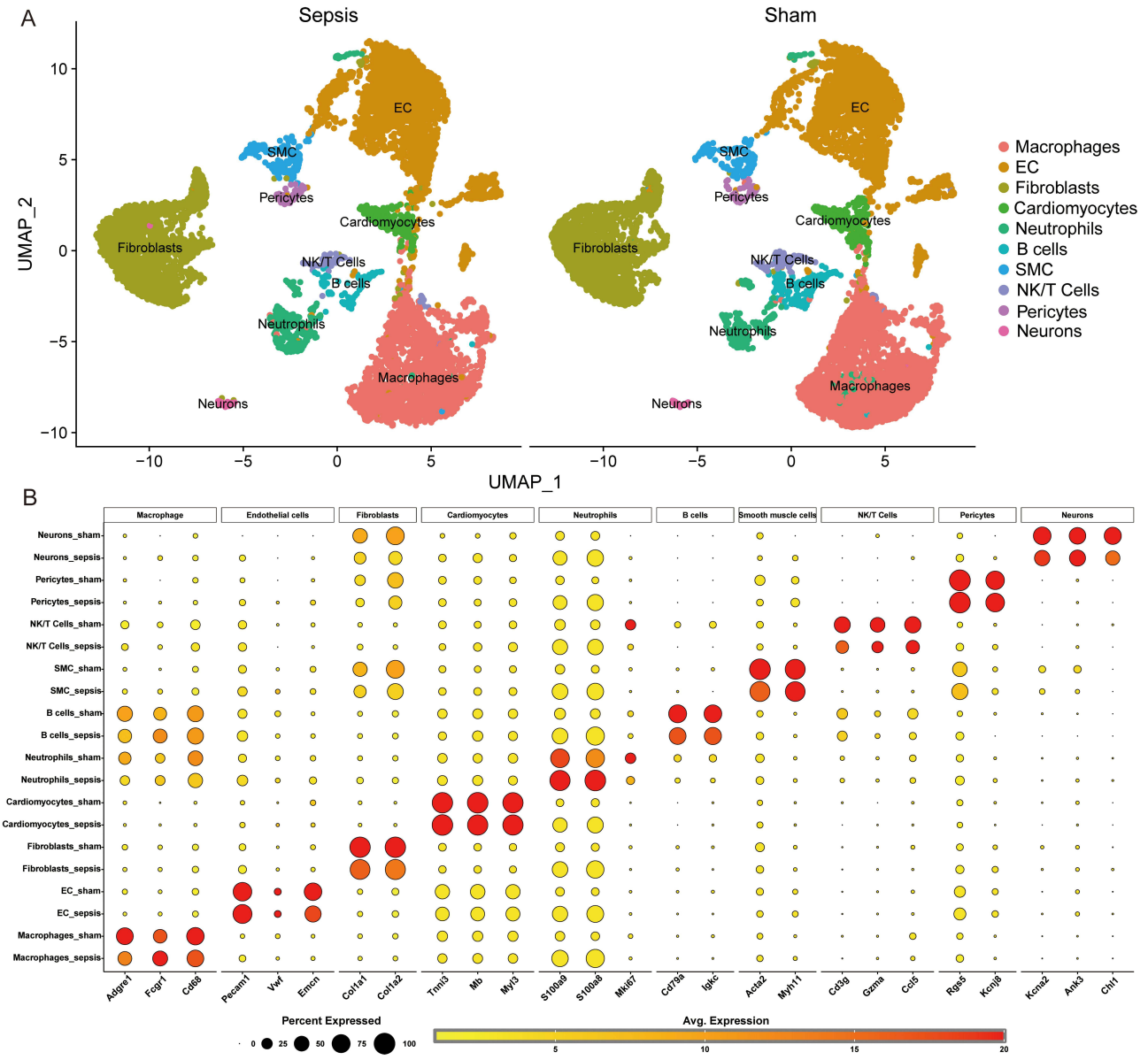

Figure 6 Dimension reduction cluster analysis and enrichment analysis (**A**) UMAP image of cells subset clusters in sham and sepsis groups. (**B**) Optimal marker gene for cell type discrimination in single cell analyses.

proposed a hypothesis positing that sepsis in patients may be connected to the suppression of immune function. As shown in Figure 6B, we could see the expression of distinct cell types using specific markers. Simultaneously, we conducted a single-cell analysis of the identified bub gene and confirmed the meaningful expression of nine genes. Additionally, we employed UMAP for visual analysis. Our findings revealed that the expressions of Cd14, Gbp2, Ifit2, and Cxcl1 were all elevated in sepsis. Cd14 was found to be increased in macrophages, neutrophils, and B cells, while the expression of Gbp2, Ifit2, and Cxcl1 in endothelial cells and fibrocytes showed significant variations in sepsis. Moreover, Cxcl1 exhibited a significant increase in B cells and smooth muscle cells, but a decrease in pericytes and neurons. These findings provided additional evidence for the significance of the genes under investigation, implying their potential regulatory role in septic cardiomyopathy (Figure 7A and B).

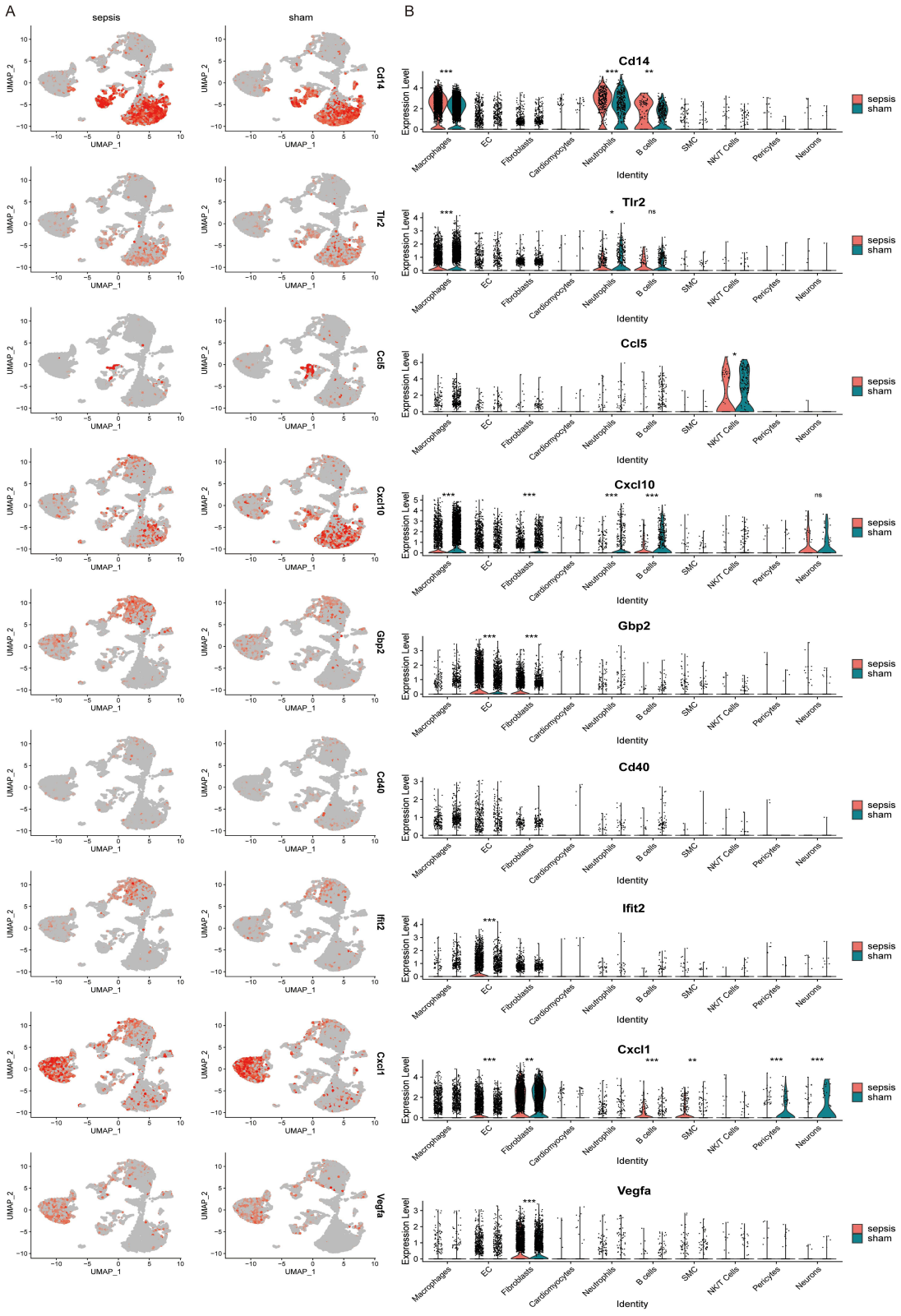

Figure 7 (**A**) UMAP images of the nine hub genes showing the expression distribution of genes in different cell types. (**B**) The expression of the nine hub genes in different cell types in sepsis and sham groups. *$p < 0.05$; **$p < 0.01$; ***$p < 0.001$.

Identification of the Transcription Factors (TF)

As previously stated, the induction of SCM resulted in differential expression of nine genes. To investigate potential regulatory mechanisms, the TRRUST database was utilized. The nine genes were screened and input into TRRUST, resulting in the identification of relevant information for eight genes. The interaction between these eight genes and transcription factors was examined, and a network was constructed. Through this analysis, six transcription factors were identified, with Sp1, Irf1, Nfkb1, Stat1, Rela and Jun being determined as the key transcription factor for Cd40, Tlr2, Cxcl10, Ccl5, Cxcl1, Cd14, Gbp2, Vegfa (Figure 8A). To confirm these findings, the expression of these transcription factors was verified using qPCR and Western blotting. As shown in Figure 8B and C, two of these six transcription factors were validated to have a different expression in SCM versus the control group (all $p < 0.05$). Western blotting analysis also showed elevation of Irf1, phosphorylated STAT1 and total STAT1 protein expression in SCM group. Interestingly, the ratio of phosphorylated STAT1 to total STAT1 did not reveal a significant difference, indicating the need for further experimental validation (Figure 8D-G). As a result, we have demonstrated that the two transcription regulators Irf1 and Stat1 could directly regulate transcription of Gbp2, Cxcl10, Ccl5 and Cd40, it might be the master regulator in SCM.

Associations Between SCM and Immune Cells Infiltration, Immune Microenvironment, and Immune Checkpoint Molecules

This article undertook an analysis of three facets of immunity, namely immune cell infiltration, immune microenvironment, and immune checkpoint molecules. The findings revealed a significant correlation between immune cell infiltration and the prognosis of various diseases. In order to investigate the relationship between SCM and immune cell infiltration

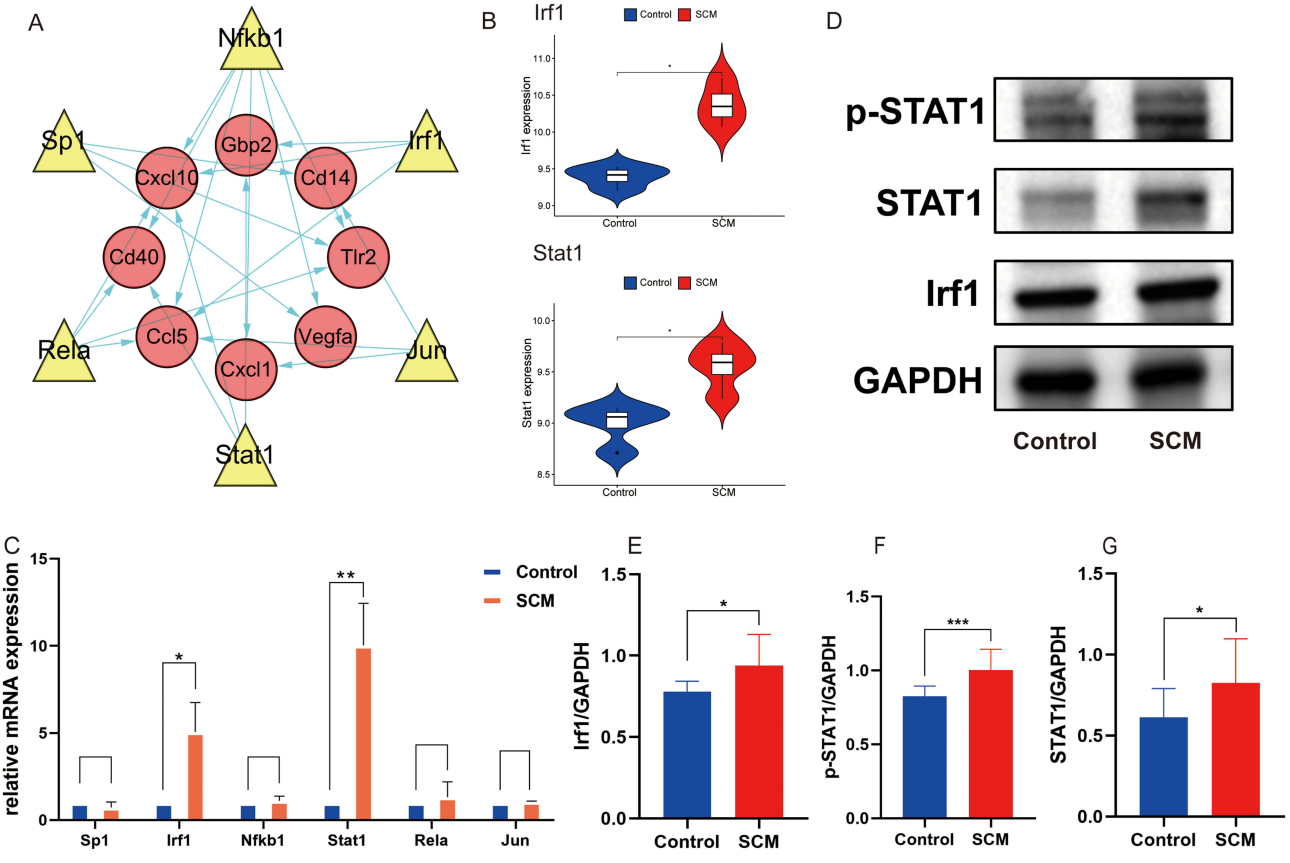

Figure 8 Identification of the transcription factors. (**A**) Transcription factors mRNA network for SCM; (**B**) Expression of Irf1 and Stat1 in the GSE53007 dataset; (**C**) Validations of the transcription factors by qPCR; (**D**) Western blotting analyses of phosphorylated STAT1, total STAT1 and IRF1; (**E-G**) Densitometric analyses of Western blotting. *$p < 0.05$; **$p < 0.01$; ***$p < 0.001$.

levels, the proportions of 25 types of immune cell infiltration levels were displayed using CIBERSORT, in four normal heart samples and four SCM mouse heart tissue samples (Figure 9A). Furthermore, the study presented various manifestations of 25 distinct types of immune cell infiltration levels in both the control and SCM groups, as depicted in Figure 9B. The findings suggested that elevated expression levels of these molecules, especially the mast cells, eosinophil cells, T cells CD8 naive, M1 macrophage, T cells CD4 follicular and NK active, may facilitate immune cell infiltration and result in an unfavorable prognosis. Notably, Figure 9C demonstrated a significant difference in ImmuneScore and EstimateScore, but not in StromalScore. Based on these results, it was concluded that SCM was associated with the immune microenvironment, which was further supported by the relationship between SCM and immune checkpoint molecules. Additionally, CD200, CD40 and LGALS9 were identified as a crucial immune molecule in SCM (Figure 9D).

Associations Between SCM and Ferroptosis, Pyroptosis, Cuproptosis and m6A RNA Methylation

In order to elucidate the potential mechanisms underlying SCM, we conducted an investigation into the interrelationships between SCM and ferroptosis, pyroptosis, cuproptosis, and m6A RNA methylation. Our findings indicated that 66 ferroptosis-related genes exhibited differential expression between the control and SCM groups, highlighting the significant role of ferroptosis in SCM (Figure 10A). Additionally, ten pyroptosis-related genes displayed differential expression between the control and SCM groups, underscoring the critical role of pyroptosis in SCM (Figure 10B). With regard to cuproptosis, we observed significant differential expression of ATP7A and DLAT between the control and SCM groups (Figure 10C). Furthermore, as depicted in Figure 10D, the m6A RNA methylation regulators METTL3 and RBMX exhibited significantly differential expression.

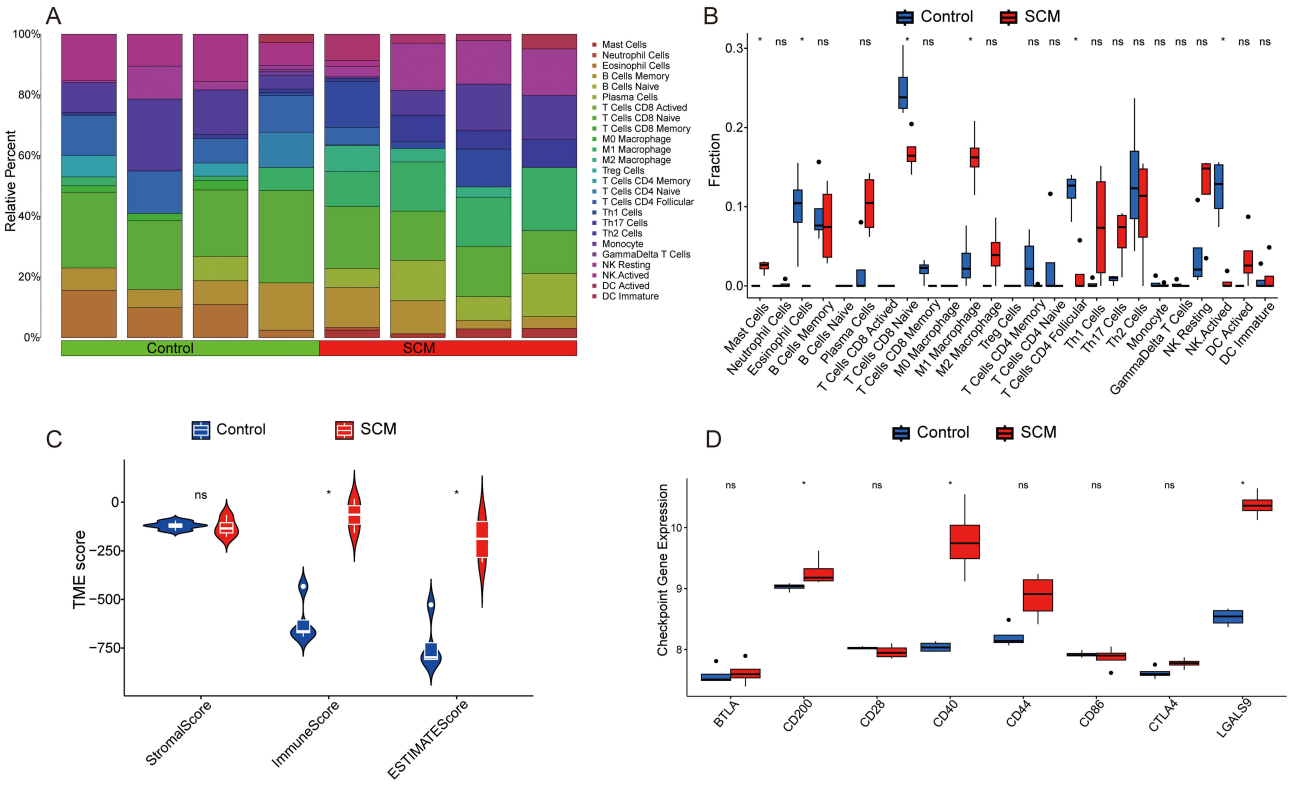

Figure 9 Associations between SCM and immunity, (**A** and **B**) Immune cells infiltration, (**C**) Immune microenvironment, and (**D**) Immune checkpoint molecules. *$p < 0.05$.

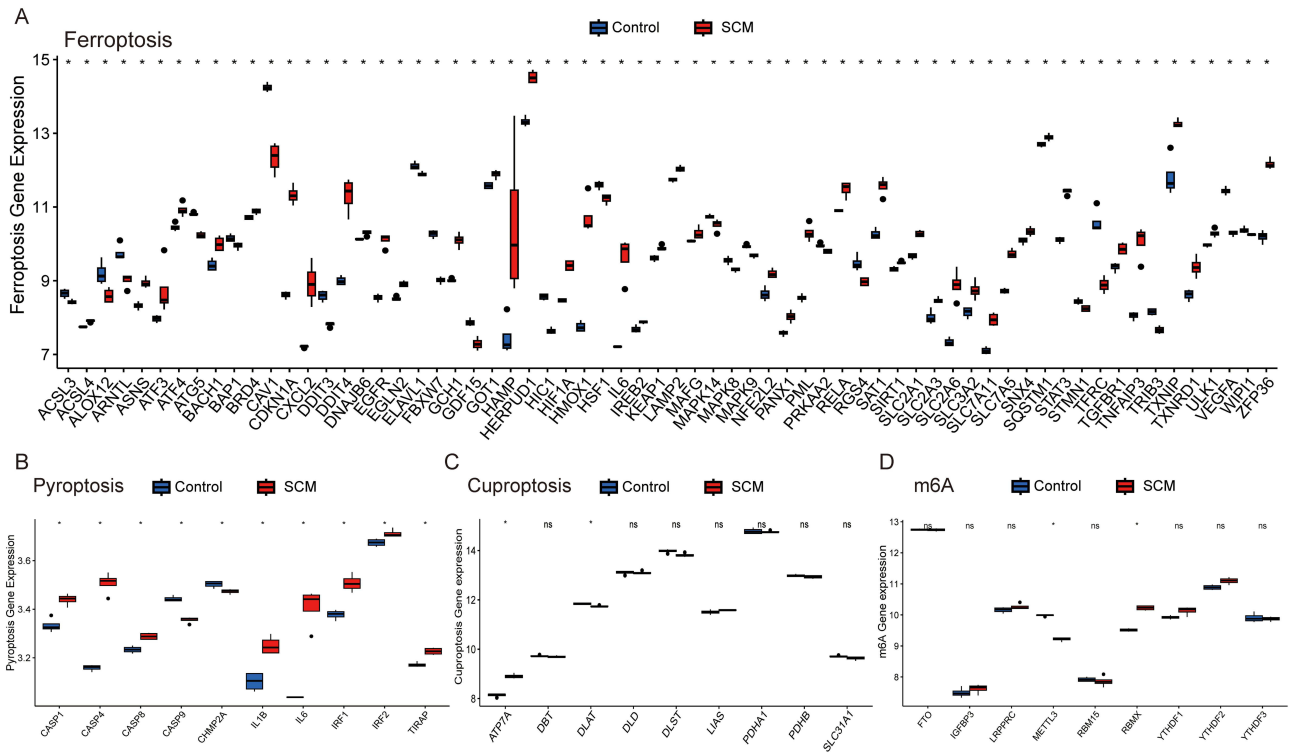

Figure 10 Associations between SCM and (**A**) Ferroptosis, (**B**) Pyroptosis, (**C**) Cuproptosis, and (**D**) m6A RNA methylation. *$p < 0.05$.

Discussion

Septic cardiomyopathy is a critical condition characterized by cardiac dysfunction arising from sepsis. Our findings highlighted the significant relationship between SCM and hub genes, including Cd40, Tlr2, Cxcl10, Ccl5, Cxcl1, Cd14, Gbp2, Ifit2, and Vegfa. Each of these genes played a crucial role in the inflammatory response and immune regulation, which was pivotal in the pathophysiology of SCM.

Toll-like receptors (Tlrs) were pattern recognition receptors of utmost importance in the innate immune system, capable of reacting to pathogen-associated molecular patterns (PAMPs) and damage-associated molecular patterns (DAMPs), thereby serving as the initial line of defense against infection and damage. Among the Toll-like receptors, Tlr2 exhibited the broadest range of expression and had the most identified ligands and its biological mechanism plays a crucial role in anti-infection immunity.[17,18] Upon infecting $Tlr2^{-/-}$ mice with sepsis, a significant decrease in mortality and improvement in cardiac function was observed in comparison to wild-type mice. These findings suggested that Tlr2 might have a regulatory function in septic cardiomyopathy,[19] which was in line with the trend of hub genes identified by our research.

Chemokines refer to a broad category of chemotactic cytokines or signaling proteins that facilitated the movement of cells to specific sites, thereby triggering biological effects. Extensive research had been conducted on various chemokines, revealing their distinct roles in inflammation, autoimmune diseases, fibrosis, tumors, and other areas.[20–22] Chemokines were classified into four subfamilies based on the arrangement of the N-terminal two cysteine residues, namely CXC, CC, (X)C, and CX3C.[23] The present study identified varying degrees of increase in Cxcl1, Cxcl10, and Ccl5 within the chemokine family. Cxcl1, as a biomarker of inflammation, exhibited elevated levels during tissue inflammation and facilitates the infiltration of neutrophils and monocytes, thereby amplifying the inflammatory response.[24] With respect to cardiovascular disorders, Cxcl1 has been linked to the advancement of atherosclerosis,[25] myocardial hypertrophy,[26] and other ailments. Cxcl10 played a pivotal role in the activation of CXCR3, a key regulator of lymphocyte transport and activation. In the context of CLP-induced septic shock, there was a significant upregulation of Cxcl10 in both plasma and the abdominal cavity. Following Cxcl10 gene knockout, there was a notable decrease in the expression of plasma inflammatory factors and the

activity of natural killer cells.[27] Furthermore, Cxcl10 exerted its influence on the NF-κB signaling pathway to disrupt the inflammatory process in vivo during the development of sepsis in mice.[28] Ccl5, like other chemokines, was involved in regulating the occurrence of inflammatory response. In sepsis model mice, the levels of Ccl5 is significantly up-regulated. The abnormal increasing of Ccl5 during sepsis accelerated the development of inflammation.[29] During normal physiological conditions, interferon-induced protein with tetratricopeptide repeats 1 gene (Ifit1) expression was not observed in the majority of cells. However, its transcription could be induced by interferon, viral infection, or LPS. Studies have revealed a significant up-regulation of Ifit1 mRNA levels in M1-polarized macrophages, suggesting a plausible correlation between Ifit1 and inflammation.[30] Gbp2, a member of the guanylate binding protein group,[31] has been recognized as an interferon-induced protein that had a vital function in pathogen infection within host defense cells in recent studies.[32] In response to bacterial invasion, Gbp2 triggered non-classical inflammasome-mediated immune responses by activating caspase-11 and caspase-4, thereby facilitating inflammasome activation in the host as a defense mechanism against bacterial infection.[33,34] The main biological role of leukocyte differentiation antigen 14 (Cd14) was to function as a receptor for lipopolysaccharide complexes, thereby facilitating their identification and attachment. Additionally, this glycoprotein receptor possessed the ability to recognize and binded to both gram-negative and gram-positive bacteria, as well as other substances, and played a critical role in pathological responses such as inflammation and endotoxin shock.[35] The transmembrane protein known as leukocyte differentiation antigen 40 (Cd40) was classified within the tumor necrosis factor receptor superfamily. Its ligand, Cd40L, was expressed on activated platelets and leukocytes. Additional investigation was needed to explore the potential effectiveness of Cd40L pathway blockers as a therapeutic approach for cardiovascular disease.[36] Vascular endothelial growth factor A (Vegfa) was widely recognized as a crucial modulator of angiogenesis, stimulating the proliferation, migration, and tubulogenesis of vascular endothelial cells. Previous investigations have demonstrated that Vegfa expression was upregulated in septic patients,[37] however, our findings indicated a downregulation of Vegfa in the context of SCM. While initial studies proposed a pathological resemblance between subclinical myocardial injury and coronary artery disease, a significant study has revealed that patients with established septic shock display enhanced coronary perfusion.[38] The aforementioned observation suggested that the development of septic cardiomyopathy might be different from the typical ischemic heart disease, potentially explaining the observed decrease in vegfa expression. Nevertheless, further empirical investigations were warranted to validate the potential role of Vegfa in promoting angiogenesis during the recuperation phase in patients with SCM.

We used the TRRUST database to explore how the nine genes might be regulated. After verifying by qPCR, we have demonstrated that the two transcription regulators Irf1 and Stat1 could directly regulate transcription of Gbp2, Cxcl10, Ccl5 and Cd40, it might be the master regulator in SCM. Stat1 played a vital role in signal transduction and was ubiquitously found in diverse tissues and cells. Its primary function entailed enhancing the expression of cell adhesion factors, thereby amplifying the inflammatory response of lymphocytes.[39,40] Stat1 as a key mediator that facilitated signal transduction between a multitude of cell membrane receptors and specific effectors. The recombinant interferon regulatory factor 1 (Irf1), an essential transcription factor, has been recognized for its substantial involvement in cellular immunity, cytokine synthesis, and cellular differentiation.[41,42] The upregulation of Irf1 within the organism elicited the secretion of diverse inflammatory factors, thereby contributing to immune and inflammatory responses.[43] This interaction could influence the progression of septic cardiomyopathy, and we look forward to our subsequent studies. A deeper investigation into this mechanism would contribute to understanding the pathophysiology of sepsis and providing new insights for future therapeutic strategies. Our research suggested an interaction between STAT1 and Irf1, which might jointly regulate the expression of antimicrobial response genes such as GBP2, CXCL10, CCL5, and CD40.[44] Our investigation revealed elevated levels of these transcription factors in SCM, suggesting that their interaction might influence the disease's progression, prompt us to pursue further studies on this mechanism.

An increasing number of researchers were exploring the connections between tumors and immunity to identify innovative treatment strategies. However, no studies have yet examined the relationship between septic cardiomyopathy and immunity. This article analyzed three aspects of immunity: immune cell infiltration, immune microenvironment, and immune checkpoint molecules. Notably, partial associations were found between SCM and 25 immune cell infiltrations, particularly involving mast cells and M1 macrophages, which played a crucial role in sepsis.[45] In recent years, an increasing number of researchers have investigated the role of cardiac immune cells in the development of cardiovascular diseases. Under septic conditions, immune cells like macrophages and T cells significantly infiltrated the heart, interacting within the cardiac microenvironment and affecting cardiomyocyte function and survival.[46] For instance, cardiac

macrophages regulated inflammation by secreting cytokines, which could promote repair or lead to fibrosis.[47] Furthermore, immune checkpoint molecules were vital in modulating immune responses,[48] potentially influencing the prognosis of patients with septic cardiomyopathy. The relationship between septic cardiomyopathy and various regulated cell death forms, such as ferroptosis, cuproptosis, pyroptosis and m6A RNA methylation was an emerging research area that underscores the complex interactions between cellular mechanisms and cardiovascular health. Notably, ferroptosis was a newly identified form of programmed cell death linked to various diseases, especially cardiovascular disease.[49] The buildup of reactive oxygen species and depletion of antioxidant defenses could trigger ferroptosis, worsening myocardial injury. Pyroptosis, a form of programmed cell death, involved gasdermin pore formation in the cell membrane, causing cell swelling and lysis that released pro-inflammatory cytokines. In the context of septic response, pyroptosis has been observed in cardiomyocytes within the myocardium.[50] Interestingly, inhibiting pyroptosis has been demonstrated to have a cardioprotective effect against myocardial dysfunction.[51] Moreover, the role of m6A RNA methylation in regulating gene expression linked to cell death pathways has garnered attention.[52] Lastly, cuproptosis, a newly identified form of programmed cell death linked to copper accumulation, was being investigated in relation to cardiovascular diseases.[53]

In summary, the relationship between septic cardiomyopathy and various regulated cell death modalities underscored the need for further research to elucidate these mechanisms and their potential as therapeutic targets for septic cardiac dysfunction. Such studies not only enhanced our understanding of the pathological mechanisms underlying septic cardiomyopathy but also offered new insights for improving patient treatment.

Limitation

This study just validated the expression of hub genes and transcription factors but did not investigate their interactions. Therefore, further experiments are necessary to validate our findings.

Conclusion

In this study, we identified nine genes (Cd40, Tlr2, Cxcl10, Ccl5, Cxcl1, Cd14, Gbp2, Ifit2, Vegfa) as hub biomarkers in the SCM model and evaluated the hub gene expression in immune cells and predicted the response to immunotherapy by single-cell analysis, which might serve as potential targets for future research. Additionally, we discovered two transcription regulators (Irf1 and Stat1) that might play a crucial role in regulating the expression of Gbp2, Cxcl10, Ccl5 and Cd40, potentially serving as the master regulator in SCM. Furthermore, our investigation into the relationship between SCM and processes such as immunity, ferroptosis, pyroptosis, cuproptosis, and m6A modification established a foundation for early screening, diagnosis, and treatment of SCM. These findings enhanced our understanding of SCM's underlying mechanisms and paved the way for novel therapeutic strategies to improve clinical outcomes.

Data Sharing Statement

Gene sequencing data were downloaded from Gene Expression Omnibus (GEO) dataset (GSE53007 and GSE207363; https://www.ncbi.nlm.nih.gov/geo/).

Ethics Approval and Consent to Participate

The study was performed with the approval of the Animal Ethics Committee of Shanghai General Hospital (Shanghai, China) (IACUC:2023AW011). The welfare of the laboratory animals was followed by guidelines for the ethical review of laboratory animal welfare People's Republic of China National Standard (GB/T 35892-2018).

Author Contributions

All authors made a significant contribution to the work reported, whether that is in the conception, study design, execution, acquisition of data, analysis and interpretation, or in all these areas; took part in drafting, revising or critically reviewing the article; gave final approval of the version to be published; have agreed on the journal to which the article has been submitted; and agree to be accountable for all aspects of the work.

Funding

This article was funded by National Natural Science Foundation of China (No.82070335 to J. Hong), the Foundation of Songjiang District Science and Technology (No.2020sjkjgg70 to J. Hong) and the Foundation of Affiliated Hospital of Xuzhou Medical University (Grant No. 2020KC003 to D.D Zhao).

Disclosure

The authors declare no competing interests in this work.

References

1. Reinhart K, Daniels R, Kissoon N, Machado FR, Schachter RD, Finfer S. Recognizing sepsis as a global health priority - A WHO resolution. *N Engl J Med*. 2017;377(5):414–417. doi:10.1056/NEJMp1707170
2. Lu NF, Jiang L, Zhu B, et al. Elevated plasma histone H4 levels are an important risk factor in the development of septic cardiomyopathy. *Balkan Med J*. 2020;37(2):72–78. doi:10.4274/balkanmedj.galenos.2019.2019.8.40
3. Lin H, Wang W, Lee M, Meng Q, Ren H. Current status of septic cardiomyopathy: basic science and clinical progress. *Front Pharmacol*. 2020;11:210. doi:10.3389/fphar.2020.00210
4. Gong Y, Zhu W, Sun M, Shi L. Bioinformatics analysis of long non-coding RNA and related diseases: an overview. *Front Genet*. 2021;12:813873. doi:10.3389/fgene.2021.813873
5. Wang YC, Wu Y, Choi J, et al. Computational genomics in the era of precision medicine: applications to variant analysis and gene therapy. *J Pers Med*. 2022;12(2):175. doi:10.3390/jpm12020175
6. Edgar R, Domrachev M, Lash AE. Gene Expression Omnibus: NCBI gene expression and hybridization array data repository. *Nucleic Acids Res*. 2002;30(1):207–210. doi:10.1093/nar/30.1.207
7. Chen M, Kong C, Zheng Z, Li Y. Identification of biomarkers associated with septic cardiomyopathy based on bioinformatics analyses. *J Comput Biol*. 2020;27(1):69–80. doi:10.1089/cmb.2019.0181
8. Lu F, Hu F, Qiu B, Zou H, Xu J. Identification of novel biomarkers in septic cardiomyopathy via integrated bioinformatics analysis and experimental validation. *Front Genet*. 2022;13:929293. doi:10.3389/fgene.2022.929293
9. Szklarczyk D, Franceschini A, Wyder S, et al. STRING v10: protein-protein interaction networks, integrated over the tree of life. *Nucleic Acids Res*. 2015;43(Database issue):D447–452. doi:10.1093/nar/gku1003
10. Alderden J, Pepper GA, Wilson A, et al. Predicting pressure injury in critical care patients: a machine-learning model. *Am J Crit Care*. 2018;27(6):461–468. doi:10.4037/ajcc2018525
11. Li F, Zhang Y, Peng Z, Wang Y, Zeng Z, Tang Z. Diagnostic, clustering, and immune cell infiltration analysis of m6A regulators in patients with sepsis. *Sci Rep*. 2023;13(1):2532. doi:10.1038/s41598-022-27039-4
12. Sheridan RP, Wang WM, Liaw A, Ma J, Gifford EM. Extreme gradient boosting as a method for quantitative structure-activity relationships. *J Chem Inf Model*. 2016;56(12):2353–2360. doi:10.1021/acs.jcim.6b00591
13. Han H, Cho JW, Lee S, et al. TRRUST v2: an expanded reference database of human and mouse transcriptional regulatory interactions. *Nucleic Acids Res*. 2018;46(D1):D380–D386. doi:10.1093/nar/gkx1013
14. Yang Y, Xie L, Peng Y, et al. Single-cell transcriptional profiling reveals low-level tragus stimulation improves sepsis-induced myocardial dysfunction by promoting M2 macrophage polarization. *Oxid Med Cell Longev*. 2022;2022:3327583. doi:10.1155/2022/3327583
15. Newman AM, Liu CL, Green MR, et al. Robust enumeration of cell subsets from tissue expression profiles. *Nat Methods*. 2015;12(5):453–457. doi:10.1038/nmeth.3337
16. Chen J, Lv B, Zhan Y, et al. Comprehensive exploration of tumor microenvironment modulation based on the ESTIMATE algorithm in bladder urothelial carcinoma microenvironment. *Front Oncol*. 2022;12:724261. doi:10.3389/fonc.2022.724261
17. Huggins MA, Sjaastad FV, Pierson M, et al. Microbial exposure enhances immunity to pathogens recognized by TLR2 but increases susceptibility to cytokine storm through TLR4 sensitization. *Cell Rep*. 2019;28(7):1729–1743e1725. doi:10.1016/j.celrep.2019.07.028
18. Kagan JC, Medzhitov R. Phosphoinositide-mediated adaptor recruitment controls Toll-like receptor signaling. *Cell*. 2006;125(5):943–955. doi:10.1016/j.cell.2006.03.047
19. Zou L, Feng Y, Chen YJ, et al. Toll-like receptor 2 plays a critical role in cardiac dysfunction during polymicrobial sepsis. *Crit Care Med*. 2010;38(5):1335–1342. doi:10.1097/CCM.0b013e3181d99e67
20. Li J, Byrne KT, Yan F, et al. Tumor cell-intrinsic factors underlie heterogeneity of immune cell infiltration and response to immunotherapy. *Immunity*. 2018;49(1):178–193e177. doi:10.1016/j.immuni.2018.06.006
21. Ogawa R, Yamamoto T, Hirai H, et al. Loss of SMAD4 promotes colorectal cancer progression by recruiting tumor-associated neutrophils via the CXCL1/8-CXCR2 Axis. *Clin Cancer Res*. 2019;25(9):2887–2899. doi:10.1158/1078-0432.CCR-18-3684
22. Wang N, Liu W, Zheng Y, et al. CXCL1 derived from tumor-associated macrophages promotes breast cancer metastasis via activating NF-kappaB/SOX4 signaling. *Cell Death Dis*. 2018;9(9):880. doi:10.1038/s41419-018-0876-3
23. Zlotnik A, Yoshie O. The chemokine superfamily revisited. *Immunity*. 2012;36(5):705–716. doi:10.1016/j.immuni.2012.05.008
24. De Filippo K, Dudeck A, Hasenberg M, et al. Mast cell and macrophage chemokines CXCL1/CXCL2 control the early stage of neutrophil recruitment during tissue inflammation. *Blood*. 2013;121(24):4930–4937. doi:10.1182/blood-2013-02-486217
25. Nencioni A, da Silva RF, Fraga-Silva RA, et al. Nicotinamide phosphoribosyltransferase inhibition reduces intraplaque CXCL1 production and associated neutrophil infiltration in atherosclerotic mice. *Thromb Haemost*. 2014;111(2):308–322. doi:10.1160/TH13-07-0531
26. Wang L, Zhang YL, Lin QY, et al. CXCL1-CXCR2 axis mediates angiotensin II-induced cardiac hypertrophy and remodelling through regulation of monocyte infiltration. *Eur Heart J*. 2018;39(20):1818–1831. doi:10.1093/eurheartj/ehy085
27. Herzig DS, Luan L, Bohannon JK, Toliver-Kinsky TE, Guo Y, Sherwood ER. The role of CXCL10 in the pathogenesis of experimental septic shock. *Crit Care*. 2014;18(3):R113. doi:10.1186/cc13902

28. Thair SA, Walley KR, Nakada TA, et al. A single nucleotide polymorphism in NF-kappaB inducing kinase is associated with mortality in septic shock. *J Immunol*. 2011;186(4):2321–2328. doi:10.4049/jimmunol.1002864
29. Hwaiz R, Rahman M, Syk I, Zhang E, Thorlacius H. Rac1-dependent secretion of platelet-derived CCL5 regulates neutrophil recruitment via activation of alveolar macrophages in septic lung injury. *J Leukoc Biol*. 2015;97(5):975–984. doi:10.1189/jlb.4A1214-603R
30. Huang C, Lewis C, Borg NA, et al. Proteomic identification of interferon-induced proteins with tetratricopeptide repeats as markers of M1 macrophage polarization. *J Proteome Res*. 2018;17(4):1485–1499. doi:10.1021/acs.jproteome.7b00828
31. MacMicking JD. Interferon-inducible effector mechanisms in cell-autonomous immunity. *Nat Rev Immunol*. 2012;12(5):367–382. doi:10.1038/nri3210
32. Praefcke GJK. Regulation of innate immune functions by guanylate-binding proteins. *Int J Med Microbiol*. 2018;308(1):237–245. doi:10.1016/j.ijmm.2017.10.013
33. Pilla DM, Hagar JA, Haldar AK, et al. Guanylate binding proteins promote caspase-11-dependent pyroptosis in response to cytoplasmic LPS. *Proc Natl Acad Sci U S A*. 2014;111(16):6046–6051. doi:10.1073/pnas.1321700111
34. Lagrange B, Benaoudia S, Wallet P, et al. Human caspase-4 detects tetra-acylated LPS and cytosolic Francisella and functions differently from murine caspase-11. *Nat Commun*. 2018;9(1):242. doi:10.1038/s41467-017-02682-y
35. Khodabandehloo H, Seyyedebrahimi S, Esfahani EN, Razi F, Meshkani R. Resveratrol supplementation decreases blood glucose without changing the circulating CD14(+)CD16(+) monocytes and inflammatory cytokines in patients with type 2 diabetes: a randomized, double-blind, placebo-controlled study. *Nutr Res*. 2018;54:40–51. doi:10.1016/j.nutres.2018.03.015
36. Lievens D, Zernecke A, Seijkens T, et al. Platelet CD40L mediates thrombotic and inflammatory processes in atherosclerosis. *Blood*. 2010;116(20):4317–4327. doi:10.1182/blood-2010-01-261206
37. Smadja DM, Borgel D, Diehl JL, Gaussem P. Vascular endothelial growth factor, as compared with placental growth factor, is increased in severe sepsis but not in organ failure. *J Thromb Haemost*. 2012;10(5):974–976. doi:10.1111/j.1538-7836.2012.04680.x
38. Dhainaut JF, Huyghebaert MF, Monsallier JF, et al. Coronary hemodynamics and myocardial metabolism of lactate, free fatty acids, glucose, and ketones in patients with septic shock. *Circulation*. 1987;75(3):533–541. doi:10.1161/01.CIR.75.3.533
39. Kohanbash G, Carrera DA, Shrivastav S, et al. Isocitrate dehydrogenase mutations suppress STAT1 and CD8+ T cell accumulation in gliomas. *J Clin Invest*. 2017;127(4):1425–1437. doi:10.1172/JCI90644
40. Ballegeer M, Van Looveren K, Timmermans S, et al. Glucocorticoid receptor dimers control intestinal STAT1 and TNF-induced inflammation in mice. *J Clin Invest*. 2018;128(8):3265–3279. doi:10.1172/JCI96636
41. Deng SY, Zhang LM, Ai YH, et al. Role of interferon regulatory factor-1 in lipopolysaccharide-induced mitochondrial damage and oxidative stress responses in macrophages. *Int J Mol Med*. 2017;40(4):1261–1269. doi:10.3892/ijmm.2017.3110
42. Li XQ, Li XN, Liang JJ, et al. IRF1 up-regulates isg15 gene expression in dsRNA stimulation or CSFV infection by targeting nucleotides −487 to −325 in the 5' flanking region. *Mol Immunol*. 2018;94:153–165. doi:10.1016/j.molimm.2017.12.025
43. Karwacz K, Miraldi ER, Pokrovskii M, et al. Critical role of IRF1 and BATF in forming chromatin landscape during type 1 regulatory cell differentiation. *Nat Immunol*. 2017;18(4):412–421. doi:10.1038/ni.3683
44. Casazza RL, Lazear HM. Why Is IFN-λ Less Inflammatory? One IRF Decides. *Immunity*. 2019;51(3):415–417. doi:10.1016/j.immuni.2019.08.019
45. Chen X, Liu Y, Gao Y, Shou S, Chai Y. The roles of macrophage polarization in the host immune response to sepsis. *Int Immunopharmacol*. 2021;96:107791. doi:10.1016/j.intimp.2021.107791
46. Forte E, Furtado MB, Rosenthal N. The interstitium in cardiac repair: role of the immune-stromal cell interplay. *Nat Rev Cardiol*. 2018;15(10):601–616. doi:10.1038/s41569-018-0077-x
47. Sun K, Li YY, Jin J. A double-edged sword of immuno-microenvironment in cardiac homeostasis and injury repair. *Signal Transduct Target Ther*. 2021;6(1):79. doi:10.1038/s41392-020-00455-6
48. Martini E, Kunderfranco P, Peano C, et al. Single-cell sequencing of mouse heart immune infiltrate in pressure overload-driven heart failure reveals extent of immune activation. *Circulation*. 2019;140(25):2089–2107. doi:10.1161/CIRCULATIONAHA.119.041694
49. Fang X, Wang H, Han D, et al. Ferroptosis as a target for protection against cardiomyopathy. *Proc Natl Acad Sci U S A*. 2019;116(7):2672–2680. doi:10.1073/pnas.1821022116
50. Li N, Zhou H, Wu H, et al. STING-IRF3 contributes to lipopolysaccharide-induced cardiac dysfunction, inflammation, apoptosis and pyroptosis by activating NLRP3. *Redox Biol*. 2019;24:101215. doi:10.1016/j.redox.2019.101215
51. Liu J, Zhao N, Shi G, Wang H. Geniposide ameliorated sepsis-induced acute kidney injury by activating PPARgamma. *Aging (Albany NY)*. 2020;12(22):22744–22758. doi:10.18632/aging.103902
52. Zhu S, Wang K, Yu Z, et al. Pulsatile flow increases METTL14-induced m 6 A modification and attenuates septic cardiomyopathy: an experimental study. *Int J Surg*. 2024;110(7):4103–4115. doi:10.1097/JS9.0000000000001402
53. Chen C, Wang J, Zhang S, et al. Epigenetic regulation of diverse regulated cell death modalities in cardiovascular disease: insights into necroptosis, pyroptosis, ferroptosis, and cuproptosis. *Redox Biol*. 2024;76:103321. doi:10.1016/j.redox.2024.103321